Journal of Nuclear Medicine, published on April 7, 2016 as doi:10.2967/jnumed.115.161513

Modulation of abnormal metabolic brain networks by experimental therapies in a nonhuman primate model of Parkinson's disease: an application to human retinal pigment epithelial (hRPE) cell implantation

Shichun Peng [1, †], Yilong Ma [1, †, *], Joseph Flores [2], Michael Cornfeldt [3], Branka Mitrovic [4, §], David Eidelberg [1, ‡], Doris J. Doudet [2, ‡]

[1] Center for Neurosciences, The Feinstein Institute for Medical Research, Manhasset, New York 11030, USA

[2] Department of Neurology, University of British Columbia, Vancouver, BC, V2Z 2J9 Canada

[3] Titan Pharmaceuticals Inc, Somerville, New Jersey 08876, USA

[4] Bayer HealthCare Pharmaceuticals Inc, Richmond, California 94806, USA

[†] These authors have contributed equally to this work.

[‡] Shared senior authorship

[§] Present address: Vertex Pharmaceuticals, Inc. San Diego, CA 92121

Running title: Metabolic network modulation by hRPE Cell Implantation

[*]Address correspondence and reprint requests to:

Name: Yilong Ma, PhD
Address: The Feinstein Institute for Medical Research
350 Community Drive, Manhasset, NY 11030
Phone: 001- (516) 562-1057
Fax: 001- (516) 562-1008
Email: yma@nshs.edu

Abstract

Abnormal covariance pattern of regional metabolism associated with Parkinson's disease (PD) is modulated by dopaminergic pharmacotherapy. Using high resolution FDG PET and network analysis we previously derived and validated a parkinsonism-related metabolic pattern (PRP) in non-human primate models of PD. It is currently not known whether this network is modulated by experimental therapeutics. In this study we examined changes in network activity by striatal implantation of human levodopa-producing retinal pigment epithelial (hRPE) cells in parkinsonian macaques and evaluated its reproducibility in a small test-retest study.

Methods PET FDG scans were acquired in eight healthy macaques and eight macaques with MPTP-induced bilateral nigrostriatal dopaminergic lesions following unilateral putaminal implantation of hRPE cells or sham surgery. PRP activity was measured prospectively in all animals and in a subset of test-retest animals using a network quantification approach. Network activity and regional metabolic values were compared on a hemispheric basis between animal groups and treatment conditions.

Results All individual macaques had sustained clinical improvement after hRPE-implantation compared to the sham surgery. PRP activity was elevated in the untreated MPTP hemispheres relative to those of the normal controls ($P < 0.00005$) but was reduced ($P < 0.05$) in the hRPE-implanted hemispheres. The modulation observed in network activity was supported by concurrent local and remote changes in regional glucose metabolism. PRP activity remained unchanged in the untreated MPTP hemispheres versus the sham-operated hemispheres. PRP activity was also stable ($P \geq 0.29$) and correlated ($R^2 \geq 0.926$; $P < 0.00005$) in the test-retest hemispheres. These findings were highly reproducible across several PRP topographies generated in multiple cohorts of parkinsonian and healthy macaques.

Conclusion We have demonstrated long-term therapeutic effects of hRPE cell implantation in non-human primate models of PD. The implantation of such levodopa-producing cells can concurrently decrease the elevated metabolic network activity in parkinsonian brains on an individual basis. These results parallel the analogous findings reported in patients with PD undergoing levodopa therapy and other symptomatic interventions. With further validation in large samples, FDG PET imaging with network analysis may provide a viable biomarker for assessing treatment response in animal models of PD following experimental therapies.

Keywords: parkinsonism, primate model, FDG PET, network analysis, dopamine cell transplantation, retinal pigment epithelial cell

Introduction

The motor clinical manifestations of Parkinson's disease (PD) are attributed chiefly to progressive loss of nigrostriatal dopaminergic neurons. This degenerative process causes a deficiency of endogenous dopamine leading to impairment in the cortico-striato-thalamo-cortical motor circuitry. FDG PET has been widely used to study functional abnormality in this circuitry. Motor features of PD are associated with an abnormal metabolic brain network (i.e., PDRP) characterized by increased activity in pallidothalamic, pontocerebellar and motor cortical regions, and decreased activity in the posterior parieto-occipital cortices (*1-4*). The network activity measured prospectively in individual patients is increased relative to normal controls and correlates positively with the severity of motor symptoms. This network is also modulated by dopaminergic and neurosurgical treatments in PD patients (*5-7*) predicting the clinical outcome.

The non-human primate injected with 1-methyl-4-phenyl-1,2,3,6-tetrahydropyridine (MPTP) is the most common primate model of experimental parkinsonism. FDG PET is useful for quantifying specific subcortical and cortical metabolic changes in MPTP primate models as a result of neurotoxic lesions or therapeutics (*8, 9*). We derived and validated a parkinsonism-related pattern (PRP) in multiple cohorts of parkinsonian and normal monkeys (*10*). PRP was analogous to PDRP in patients in terms of topographic features, group discrimination and clinical correlation (*5, 7*). It is currently not known whether this network is modulated by experimental therapies in the MPTP primate model of PD.

Human retinal pigment epithelial (hRPE) cells of fetal origin, attached to gelatin microcarrier support matrix (MSM^{TM}: GM) (hRPE-GM) for enhanced survival, have been used as a potential therapy to reverse parkinsonian motor deficits in rodents (*11, 12*), monkeys (*13, 14*) and, under the name Spheramine®, in PD patients (*15, 16*). There is unequivocal evidence that hRPE-GM implants can survive without immunosuppression (*17, 18*) as in fetal cell transplantation in PD patients (*19*). Increased [^{18}F]fluorodopa uptake and decreased [^{11}C]raclopride binding were reported in the implanted striatum following unilateral implant of hRPE-GM in monkeys,

suggesting a dopaminergic mechanism (*14*). Despite sustained improvement in clinical motor scores over several years, these molecular markers are highly variable over the long-term due to inherent compensatory modulation following therapy and disease progression in patients (*20, 21*). FDG PET imaging may be more sensitive for examining systemic brain function recovery after dopaminergic cell implantation. However, there are presently no studies on the metabolic effects of dopaminergic implants in parkinsonian animals or patients.

In this study we describe a general approach to assessing network and regionally-specific metabolic responses to experimental therapies in non-human primate models of parkinsonism. We hypothesized that metabolic network is modulated by striatal cell implantation via widespread downstream changes in brain circuitry associated with motor function recovery. To this end we evaluated the effects of hRPE-GM implants on metabolic brain network activity and regional metabolism in parkinsonian macaques. The test-retest stability of network activity was also assessed prospectively in a small cohort.

Materials and methods

Characteristics of macaques

This study included 16 adult rhesus monkeys (male/female 14/2, age 8-22 y). Eight monkeys (age 13.5 ± 5.2 [mean ± SD] y; weight 9.1 ± 1.7 kg) developed mild to moderately severe bilateral parkinsonism following chronic intravenous administration of MPTP over several months. hRPE-GM or sham (GM only) was implanted unilaterally in the striatum in the fully recovered and stable animals (i.e. motor scores unchanged for >3-4 mo). Normal controls comprised 8 healthy monkeys (age 10.8 ± 4.7 y; weight 9.7 ± 2.7 kg) matched in age ($P = 0.28$) and weight ($P = 0.63$) to the parkinsonian animals. Clinical evaluation and FDG PET were performed in all animals and repeated in a small cohort of four subgroups (Table 1; Suppl. Tables 1-2). Part of these imaging data was used previously for the determination and validation of PRP

(*10*). All the procedures followed the Canadian Council on Animal Care Regulations and were approved by the Committee on Animal Care of the University of British Columbia.

The parkinsonian and healthy monkeys lived in groups or pairs and were able to forage and care for themselves. Motor scores of these animals were obtained using a reliable clinical rating scale (*14*), equivalent to the unified Parkinson's disease rating scale (UPDRS) with a maximal score of 26. All MPTP-lesioned animals presented bilateral parkinsonian symptoms with generally reduced activity, hypokinesia, bradykinesia, tremor and deficits in balance and coordination. The parkinsonian animals were evaluated before and 6-48 mon after unilateral striatal implantation (Fig. 1A) and rated as mild moderate (n = 7) or moderately severe (n = 1) at the time of imaging (motor score 11.9 ± 5.1; range 8-23).

Assessment of glucose metabolic networks was not part of the initial hRPE study of unilateral implantation efficacy and the animals were only scanned late in the clinical study as a proof of concept. Network activities were thus compared between implanted and non-implanted hemispheres as well as with healthy controls.

Protocols of hRPE cell preparation and implantation

The preparation of hRPE-GM and GM slurry and sterile surgical and implantation procedures were described elsewhere (*14, 17*). This study used hRPE cells from two different sources (Table 1). The initial cells provided by Titan Pharmaceuticals came from fetal donor of an age (22-24 wk) similar to those used in the small open-label clinical phase I trial (*16*). Later cells supplied by Bayer Schering Pharma came from two different neonate donors (32-34 wk) similar in age and preparation to those used in the large double-blind clinical phase II trial (*22*).

The non-immunosuppressed parkinsonian monkeys received unilateral injections of hRPE-GM (n = 6) or GM alone (n = 3) randomly in the left or right striatum. The implantation of GM was performed only in a small number of animals to confirm the finding in the original safety and efficacy study (*13*). One animal was first implanted with GM in one striatum and after several

months without notable clinical improvement, received hRPE-GM in the contralateral striatum. The animals were sedated with ketamine (10 mg/kg im) for placement of intravenous lines and intubation, and put under isoflurane anesthesia (2-3%). The animals received prophylactic antibiotics and analgesics before and after the procedure. Each animal was placed in a MRI-compatible stereotaxic frame with the implant coordinates determined from a MRI obtained immediately prior to the surgery. Each animal received 5 tracks, 2 mm apart, in a zig-zag pattern covering the extent of putamen or posterior caudate/putamen. Fifty μL of slurry with 65,000 to 100,000 hRPE cells attached to GM or GM alone were injected in each track. No adverse events were observed in any of the animals after hRPE-GM or sham implantation.

PET imaging

PET imaging was performed using a high resolution research tomograph (HRRT, CPS Innovations, Knoxville, TN) with a 3D resolution of 2.5 mm (*10*). The monkey and his/her partner were moved to smaller squeeze cages in an adjacent room to facilitate radiotracer administration. FDG (148-222 MBq) was injected intramuscularly in the left or right thigh. The animals stayed awake during an uptake period of 40-45 min and none exhibited abnormal behavior or marked motor activity in video recording. The monkey was then rapidly anesthetized (ketamine followed by isoflurane for maintenance). A 30 min emission scan followed by a 10 min attenuation scan were acquired from 80 min post-injection and reconstructed using the ordered subsets expectation maximization algorithm. There were no differences in injected dose (211.4 ± 22.7 vs 207.7 ± 41.5 MBq; $P = 0.83$) and blood glucose (3.96 ± 0.52 vs 3.81 ± 0.39 mmol/L; $P = 0.52$) values between the healthy and all parkinsonian animals (Table 1; Suppl. Table 1).

Image processing

Image processing was performed with in-house program (ScanVP available at http://www.feinsteinneuroscience.org) and statistical parametric mapping software (SPM;

Institute of Neurology, London, UK). PET images were spatially normalized into a macaque brain template (*23*) and smoothed with a 4 mm Gaussian filter. To assess the metabolic effects of unilateral implants these images were separated into hemispheres and flipped onto the same side. The left and right hemispheric images were averaged for the animals that were healthy or had only bilateral MPTP lesions. This made the number of hemispheres in the analysis equal to that of animals (Fig. 2).

Reproducible PRP metabolic brain networks across animal cohorts

We previously established several metabolic patterns (PRP1 to PRP5) in two independent cohorts of parkinsonian and healthy rhesus macaques (*10*). PRPs 1-4 were generated over hemispheres. The hemispheric PRPs (i.e. PRP1) were topographically comparable to symmetrical PRP5 produced over whole brains in the parkinsonian and control animals available. These patterns corresponded to the MPTP animals with moderate to severe (PRP1, PRP2, PRP5) and mild to moderate (PRP3, PRP4) motor symptoms. All PRPs shared a similar topography characterized by positive activity in striatal, pallidothalamic, pons and motor cortical regions, and negative activity in the posterior parietal-occipital cortex (Fig. 3A; Suppl. Fig. 1A). Network activity in individual hemispheres or brains discriminated MPTP and normal animals in the derivation sample ($P < 0.005$) for each PRP (Table 2; Suppl. Fig. 3).

Changes in PRP network activity in the treatment sample

The treatment sample included the 8 MPTP monkeys unilaterally treated with hRPE-GM or GM implantation. We quantified the expression of each PRP (i.e., PRPs 1 to 5) prospectively in individual hemispheres blind to animal, clinical symptom and treatment status (*1, 4*). Network score of PRP5 was computed in the whole brains but over hemispheres in the images involving unilateral interventions such as MPTP lesion, hPRE or sham implants. All network scores were z-transformed using analogous PRP scores for the healthy animals in the derivation cohort so that

they had a mean of zero and standard deviation of one. Network scores were compared among 8 normal, 7 MPTP and 6 hRPE-implanted hemispheres.

Changes in PRP network activity in the test-retest sample

The test-retest sample included a mixed group of 7 normal, MPTP, implant and sham animals imaged twice over 0.94 ± 0.73 y (Suppl. Table 2). Animal weight, injected dose and blood glucose level did not change between the two time points ($P \geq 0.17$). Neither did motor scores in the parkinsonian animals ($P > 0.11$). Network scores of all PRPs were computed in the 9 hemispheres of the paired images with their test-retest reliability evaluated across the two normal, three MPTP, two implant and two sham hemispheres.

Regional Metabolic Effects of MPTP Administration and hRPE Cell Implantation

Differences in regional glucose metabolism were assessed *post-hoc* on a voxel basis with univariate SPM analysis. An unpaired or paired *t*-test was used to compare 7 MPTP and 8 normal scans or 6 hPRE-implanted and 6 MPTP scans respectively. Analysis of covariance was used to account for inter-individual variability in global metabolism. The differences were considered significant at $P < 0.005$ with a cluster size of 20 voxels within a PRP-defined brain mask for hypothesis testing. The resulting maps of *t*-statistic were examined to localize relevant regions anatomically in reference to a macaque brain atlas.

Statistical analysis

Unpaired *t*-tests were employed to assess differences in network activity between animal groups. Paired *t*-tests were used to compare changes in motor ratings and in network scores between the MPTP and implant hemispheres or between the test and retest scans. The relationships between these measures and their interval changes were evaluated by correlation

analysis. All analyses were performed using JMP software (Version 5, SAS Institute, CRAY, NC) and were considered significant for $P < 0.05$.

Results

Clinical improvement by hRPE-GM implantation

At the preoperative baseline, motor ratings in the parkinsonian monkeys were 19.1± 2.9 (range 14.5-22.5) and comparable in the animals with hRPE-GM or sham implants (Fig. 1A). The hRPE-GM implanted animals showed sustained motor improvement (46.7 ± 6.9% [mean ± SE]; range 23-66%; $P < 0.001$) compared to the pre-implant scores and to the animals implanted with GM carriers only (Fig. 1B). The clinical improvement was robust in four animals (fetal cells) over 3-4 y and in two animals (neonatal cells) over 6-10 mon after hRPE-GM implantation. Motor ratings showed no changes in the three GM-carriers implanted animals over 6-12 mon.

Network modulation by hRPE-GM implantation

Network activity changed in response to the implantation for PRPs 1-5 (Table 2; Fig. 3B; Suppl. Fig. 1B). In the 7 monkeys with unilateral implants, network scores were elevated in the untreated MPTP hemispheres relative to the normal values ($P < 0.00005$) but lower (10.9-26.8 %, $P < 0.05$; n = 6) in the hRPE-GM implanted versus the untreated MPTP hemispheres. Network scores in the hRPE-GM-implanted hemispheres were still higher than the normal values ($P < 0.005$). Network activity did not change in the three sham-operated animals (Suppl. Fig. 4). Treatment-mediated changes in network activity and clinical outcome did not correlate ($R^2 \leq 0.18$, $P \geq 0.25$) across the implant and sham-operated animals.

Metabolic Differences between Normal, Parkinsonian and RPE-implanted Macaques

Hemispheric global metabolic values (in kBq/mL) did not change between the groups (8 Normal: 46.0 ± 6.4; 7 MPTP: 54.6 ± 3.5 [mean ± SE]; $P = 0.28$) or conditions (6 MPTP: 52.5 ±

4.4; 6 hPRE-implant: 47.5 ± 6.7, $P = 0.21$). Comparing the MPTP-lesioned to the normal hemispheres, glucose metabolism increased in the putamen/pallidum, thalamus, pons, medial frontal gyrus/cingulate, sensorimotor cortex (SMC) and supplementary motor area (SMA) but decreased in smaller areas in the posterior parieto-occipital cortex (Fig. 4A; Table 3). Concurrently, glucose metabolism decreased in the same set of hypermetabolic regions but did not increase in the hPRE-implanted versus the MPTP-lesioned hemispheres (Fig. 4B; Table 3).

Test-retest reproducibility of network activity

Network scores in the test/retest images remained unchanged ($P \geq 0.29$) and were strongly correlated ($R^2 \geq 0.926$, $P < 0.00001$) in the hemispheres of normal, MPTP, implanted and sham-operated animals (Fig. 5; Suppl. Fig. 2). The results were similar across PRPs 1 to 5.

Discussion

Measurement of regional glucose metabolism with FDG PET has been used extensively to assess the local and remote functional consequences of therapeutics in neurodegenerative disorders. This was shown by gene therapy in parkinsonian macaques (*9*) and cellular-based therapies in patients with multiple system atrophy (*24*) as well as in primate models of intracerebral hematoma (*25*) and rat models of cerebral ischemia (*26*). These studies documented widely-distributed metabolic changes on a regional level but did not provide valuable information on a system-level. We describe a complementary method of measuring both system and regional changes for evaluating treatment-mediated modulation of parkinsonism-related metabolic brain networks in primate models of PD.

In this study we reported long-term effects of implanting hRPE-GM in MPTP-treated rhesus monkeys. Consistent motor recovery was present in the animals with unilateral hRPE-GM implants that remained stable over 36-48 mon but absent in those with GM only (Fig. 1B). This

sustained improvement is very similar to the predominantly contralateral improvements in off-state UPDRS motor scores over 48 or 36 mon in PD patients implanted unilaterally with Spheramine (*16*) and hRPE-derived dopaminergic cells alone (*27*). Elevated PRP activity was significantly lower in the hRPE-GM-implanted versus the untreated MPTP hemispheres (Fig. 3B) but did not change in the sham-operated hemispheres (Suppl. Fig. 4). This represented a robust effect of treatment given that PRP scores were elevated and highly symmetrical in bilaterally-lesioned animals without therapeutic intervention (*10*). These observations were consistently replicated for each of the five PRPs on a hemispheric or whole-brain basis.

We observed metabolic modulation in the same set of broadly-distributed brain regions underlying the topography of PRP network. The regionally-specific changes in glucose metabolism not only revealed downstream effects of MPTP lesioning and hPRE-GM implants but also explained the elevated PRP activity in parkinsonian macaques and its subsequent suppression by this cell-based therapy. Of note, the changes in regional and network metabolic activity were independent of global metabolic values which remained unchanged between animal groups or treatment conditions. The altered regional metabolism associated with the elevated PRP activity was similar in MPTP-lesioned cynomolgus monkeys scanned on a clinical PET/CT (*28*).

Importantly, the changes in network and widespread regional metabolic activity after hRPE-GM implantation agree very well with analogous observations in patients undergoing levodopa therapy and a variety of other neurosurgical interventions (*5-7*). These findings indicate that clinical response to symptomatic therapies is associated with the suppression of an elevated activity in PD-related brain networks in both animal models and patients. We also showed high test–retest reliability of network activity (PRPs 1-5) in individual animals, regardless of clinical phenotype and treatment status, similar to the reports in human subjects (*1*) and cynomolgus monkeys (*28*). Therefore, our cross-species studies have established that PD patients and primate models share homologous motor PD-related metabolic patterns that can be used prospectively for the assessment of disease severity and response to novel cell or gene therapies (*29, 30*).

In this study we assumed implicitly that unilateral implantation of hRPE-GM cells causes metabolic effects mainly in the ipsilateral hemisphere since these non-neuronal cells do not appear to make synaptic connections with the host brain. Indeed, hPRE-related changes in dopaminergic markers were located only in the unilaterally-implanted putamen in monkeys (*14*) and patients (*27*) along with contralateral clinical benefits. Many unilateral intervention studies make the same assumption so as to use the contralateral side as an internal control for the treatment side. The mean hemispheric difference in network activity was <6.5% in the two test-retest animals (Nos. 2-3) who received the second implants in the contralateral striatum (Suppl. File), much smaller than the effects of hRPE-GM implants (Table 2). Changes in metabolic value in remotely located regions and PDRP activity over the brain were also present only in the treated hemispheres plus improved contralateral motor ratings in PD patients following unilateral subthalamic gene therapy (*6*). All these results support the key assumption we made in this study.

The sham treatment involved only a small number of animals due to the ethical consideration of not performing invasive neurosurgery unnecessarily after we observed no clinical improvement in these animals. Our results are overall compatible with clinical findings in 6-hydroxydopamine-lesioned rats (*12*) and in the earlier blinded sham-controlled study in hemiparkinsonian rhesus monkeys (*13*) that demonstrated significant clinical improvements in the animals implanted with hPRE-GM but not with sham (needle tracks) and microcarriers alone. These studies further suggest that control animals do not develop placebo responses as patients do.

We did not detect a significant association between the degree of network modulation and the clinical outcome in the limited sample of this study, due to the narrow range and variation of hRPE-mediated changes in both motor and network scores. Several sources of variability specific to our implantation therapy are described below. Despite this added variability, it is remarkable that each animal and each hemisphere in the hRPE-GM implanted group demonstrates some level of reversal of parkinsonian attributes.

Our results revealed only a partial clinical recovery and suboptimal restoration of impaired brain circuitry by hRPE-GM implantation. This may be attributed to several factors: unilateral implantation, small numbers of implanted cells, lower rates of cell survival, poor integration with the host tissue and properties of the cells themselves. It is important to remember that the hypothesized mechanism of action of striatally-implanted hRPE cells is not the production of dopamine but constant *in situ* release of low levels of levodopa. Their therapeutic effect is thus indirect, through the increased stimulation of dopamine synthesis from surviving dopaminergic terminals, an action similar to that of orally-administered levodopa but at much lower, physiological concentrations. The incomplete functional recovery is consistent with clinical experience in patients with unilateral Spheramine implants (*15, 22*). These patients continued to receive daily levodopa treatment, albeit generally at much lower doses than before implant, to obtain optimal therapeutic benefit. Hence, neither Spheramine nor hRPE-GM cells at the concentrations given were sufficient to completely reverse the motor symptoms of parkinsonism.

It is fitting to provide some explanations for the discrepancy between our preclinical data and published clinical trial results. Motor symptoms of our monkeys were comparable to the patients in the phase I and II trials (*15, 22*) although their age ranges are closer to young patients in the phase I trial (*15*). Transplantation protocols were similar in both primates and patients with comparable numbers of tracts and cells implanted per side in the absence of immunosuppression. However, the hRPE cells used in this study were not all from the same donor and same origin (Table 1; Fig. 1). Some were comparable to the fetal cells used in the successful open-label phase I trial (*15*) while others were similar to the neonatal cells used in the phase II trial that ultimately failed to demonstrate the efficacy of this intervention over placebo (*22*). Some of the variability in the behavioral and metabolic results may stem from the difference in cell sources. Indeed, several studies have shown that fetal hRPE cells have better survival characteristics than cells obtained from older donors (*31*). In our small group of animals, it was not possible to determine if the overall behavioral improvement or PRP network recovery was driven mostly by the fetal cells

effects. Of note, homogeneity of animals and similarity of MPTP disease model are also in sharp contrast with aging PD patients suffering from multifactorial disease. One key difference in any double blind, sham-controlled preclinical or clinical study is that animals do not develop placebo effects as compared to patients undergoing the same trial.

There are several limitations in this study: (1) small sample size, particularly in sham-operated control animals; (2) unilateral implantation and subsequent analysis on a hemispheric basis; (3) variable time intervals between implantation and imaging or between test and retest scans; (4) measurement of clinical motor scores rather than the more quantitative behavioral testing of the left versus right dexterity as in the monkey movement analysis panel. FDG PET was not part of the original study design and only added after validation of the scanning procedure with glucose uptake in awake animals. Nevertheless, this study represents a simple proof of concept for the design of future preclinical trials. Within-subject designs with more potent or varied dose regimen will be necessary to delineate the effects of this or other potential therapies on metabolic network activity and correlations with behavioral outcome in a large sample before and after intervention.

Conclusion

We report the first study on the modulation of parkinsonism-related metabolic networks by experimental therapies in MPTP-treated primate models of PD. The covariance pattern of abnormal metabolism and network modulation in parkinsonian macaques parallel the reports in PD patients undergoing other symptomatic interventions. Changes in network activity may be useful for assessing the efficacy of novel therapeutics in both animal models and patients with PD. We also show a specific role of hRPE cells in the reversal of motor impairments in parkinsonian primates based on clinical benefits and suppression of network activity following implantation.

These data support the use of FDG PET to evaluate other formulations or microcarrier substrates (*32*) with hRPE-GM and other cell-based restorative therapies in patients with PD.

Disclosure

Dr. Doudet received grant-in-aid from Titan Pharmaceuticals and Bayer HealthCare Pharmaceuticals during this study but not for this study. Dr. Eidelberg serves on the scientific advisory board for and has received honoraria from the Michael J. Fox Foundation (MJFF) and The Bachmann-Strauss Dystonia and Parkinson Foundation; is listed as coinventor of patents re: Markers for use in screening patients for nervous system dysfunction and a method and apparatus for using same, without financial gain; has received research support from the NIH , High Q Foundation, the Dana Foundation, MJFF, and The Bachmann-Strauss Dystonia and Parkinson Foundation; has served as scientific advisor for the Thomas Hartman Foundation for Parkinson's Research, Inc.; and has received consultant fees from Pfizer Inc. Dr. Cornfeldt was employed by Titan Pharmaceuticals and owns stock purchased in the open market. Dr. Mitrovic was an employee of Bayer HealthCare Pharmaceuticals and is currently employed by Vertex Pharmaceuticals with stock ownership. Dr. Ma has received research support from the NIH. Other authors disclose no financial interests.

Acknowledgement

This research was supported by Team Grant (CTP-79851) at the UBC from the Canadian Institute of Health Research. The authors thank Titan Pharmaceuticals Inc and Bayer HealthCare Pharmaceuticals for their gifts of the hRPE cells and microcarriers and UBC/TRIUMF PET program for their assistance in imaging studies. Special thanks are due to the personnel of the UBC Animal Resources Unit and Animal Care Facilities for their outstanding care of the animals. The work of Drs. Peng, Ma and Eidelberg was supported by the NIH Morris K Udall Center of Excellence for Parkinson's Disease Research (P50 NS071675).

References

1. Ma Y, Tang C, Spetsieris PG, Dhawan V, Eidelberg D. Abnormal metabolic network activity in Parkinson's disease: test-retest reproducibility. *J Cereb Blood Flow Metab.* 2007;27:597-605.

2. Wu P, Wang J, Peng S, et al. Metabolic brain network in the Chinese patients with Parkinson's disease based on 18F-FDG PET imaging. *Parkinsonism Relat Disord.* 2013;19:622-627.

3. Teune LK, Renken RJ, Mudali D, et al. Validation of parkinsonian disease-related metabolic brain patterns. *Movement disorders : official journal of the Movement Disorder Society.* 2013;28:547-551.

4. Peng S, Ma Y, Spetsieris PG, et al. Characterization of disease-related covariance topographies with SSMPCA toolbox: effects of spatial normalization and PET scanners. *Human brain mapping.* 2014;35:1801-1814.

5. Asanuma K, Tang C, Ma Y, et al. Network modulation in the treatment of Parkinson's disease. *Brain.* 2006;129:2667-2678.

6. Feigin A, Kaplitt MG, Tang C, et al. Modulation of metabolic brain networks after subthalamic gene therapy for Parkinson's disease. *Proc Natl Acad Sci U S A.* 2007;104:19559-19564.

7. Eidelberg D. Metabolic brain networks in neurodegenerative disorders: a functional imaging approach. *Trends Neurosci.* 2009;32:548-557.

8. Brownell AL, Canales K, Chen YI, et al. Mapping of brain function after MPTP-induced neurotoxicity in a primate Parkinson's disease model. *Neuroimage.* 2003;20:1064-1075.

9. Emborg ME, Carbon M, Holden JE, et al. Subthalamic glutamic acid decarboxylase gene therapy: changes in motor function and cortical metabolism. *J Cereb Blood Flow Metab.* 2007;27:501-509.

10. Ma Y, Peng S, Spetsieris PG, Sossi V, Eidelberg D, Doudet DJ. Abnormal metabolic brain networks in a nonhuman primate model of parkinsonism. *J Cereb Blood Flow Metab.* 2012;32:633-642.

11. Cepeda IL, Flores J, Cornfeldt ML, O'Kusky JR, Doudet DJ. Human retinal pigment epithelial cell implants ameliorate motor deficits in two rat models of Parkinson disease. *Journal of neuropathology and experimental neurology.* 2007;66:576-584.

12. Subramanian T, Marchionini D, Potter EM, Cornfeldt ML. Striatal xenotransplantation of human retinal pigment epithelial cells attached to microcarriers in

hemiparkinsonian rats ameliorates behavioral deficits without provoking a host immune response. *Cell transplantation.* 2002;11:207-214.

13. Watts RL, Raiser CD, Stover NP, et al. Stereotaxic intrastriatal implantation of human retinal pigment epithelial (hRPE) cells attached to gelatin microcarriers: a potential new cell therapy for Parkinson's disease. *Journal of neural transmission Supplementum.* 2003:215-227.

14. Doudet DJ, Cornfeldt ML, Honey CR, Schweikert AW, Allen RC. PET imaging of implanted human retinal pigment epithelial cells in the MPTP-induced primate model of Parkinson's disease. *Exp Neurol.* 2004;189:361-368.

15. Stover NP, Bakay RA, Subramanian T, et al. Intrastriatal implantation of human retinal pigment epithelial cells attached to microcarriers in advanced Parkinson disease. *Arch Neurol.* 2005;62:1833-1837.

16. Stover NP, Watts RL. Spheramine for treatment of Parkinson's disease. *Neurotherapeutics : the journal of the American Society for Experimental NeuroTherapeutics.* 2008;5:252-259.

17. Flores J, Cepeda IL, Cornfeldt ML, O'Kusky JR, Doudet DJ. Characterization and survival of long-term implants of human retinal pigment epithelial cells attached to gelatin microcarriers in a model of Parkinson disease. *J Neuropathol Exp Neurol.* 2007;66:585-596.

18. Farag ES, Vinters HV, Bronstein J. Pathologic findings in retinal pigment epithelial cell implantation for Parkinson disease. *Neurology.* 2009;73:1095-1102.

19. Ma Y, Tang C, Chaly T, et al. Dopamine cell implantation in Parkinson's disease: long-term clinical and (18)F-FDOPA PET outcomes. *J Nucl Med.* 2010;51:7-15.

20. Nandhagopal R, Kuramoto L, Schulzer M, et al. Longitudinal evolution of compensatory changes in striatal dopamine processing in Parkinson's disease. *Brain : a journal of neurology.* 2011;134:3290-3298.

21. Pavese N, Rivero-Bosch M, Lewis SJ, Whone AL, Brooks DJ. Progression of monoaminergic dysfunction in Parkinson's disease: a longitudinal 18F-dopa PET study. *NeuroImage.* 2011;56:1463-1468.

22. Gross RE, Watts RL, Hauser RA, et al. Intrastriatal transplantation of microcarrier-bound human retinal pigment epithelial cells versus sham surgery in patients with advanced Parkinson's disease: a double-blind, randomised, controlled trial. *The Lancet Neurology.* 2011;10:509-519.

23. Black KJ, Koller JM, Snyder AZ, Perlmutter JS. Template images for nonhuman primate neuroimaging: 2. Macaque. *Neuroimage.* 2001;14:744-748.

24. Lee PH, Lee JE, Kim HS, et al. A randomized trial of mesenchymal stem cells in multiple system atrophy. *Annals of neurology.* 2012;72:32-40.

25. Feng M, Zhu H, Zhu Z, et al. Serial 18F-FDG PET demonstrates benefit of human mesenchymal stem cells in treatment of intracerebral hematoma: a translational study in a primate model. *Journal of nuclear medicine : official publication, Society of Nuclear Medicine.* 2011;52:90-97.

26. Wang J, Chao F, Han F, et al. PET demonstrates functional recovery after transplantation of induced pluripotent stem cells in a rat model of cerebral ischemic injury. *Journal of nuclear medicine : official publication, Society of Nuclear Medicine.* 2013;54:785-792.

27. Yin F, Tian ZM, Liu S, et al. Transplantation of human retinal pigment epithelium cells in the treatment for Parkinson disease. *CNS neuroscience & therapeutics.* 2012;18:1012-1020.

28. Ma Y, Johnston TH, Peng S, et al. Reproducibility of a Parkinsonism-related metabolic brain network in non-human primates: A descriptive pilot study with FDG PET. *Movement Disorders.* 2015;30:1283-1288.

29. Ma Y, Peng S, Dhawan V, Eidelberg D. Dopamine cell transplantation in Parkinson's disease: challenge and perspective. *Br Med Bull.* 2011;100:173-189.

30. Bartus RT, Baumann TL, Brown L, Kruegel BR, Ostrove JM, Herzog CD. Advancing neurotrophic factors as treatments for age-related neurodegenerative diseases: developing and demonstrating "clinical proof-of-concept" for AAV-neurturin (CERE-120) in Parkinson's disease. *Neurobiology of aging.* 2013;34:35-61.

31. Russ K, Flores J, Brudek T, Doudet D. Neonatal human retinal pigment epithelial cells secrete limited trophic factors in vitro and in vivo following striatal implantation in parkinsonian rats. *Journal of neural transmission.* 2015.

32. Falk T, Congrove NR, Zhang S, McCourt AD, Sherman SJ, McKay BS. PEDF and VEGF-A output from human retinal pigment epithelial cells grown on novel microcarriers. *Journal of biomedicine & biotechnology.* 2012;2012:278932.

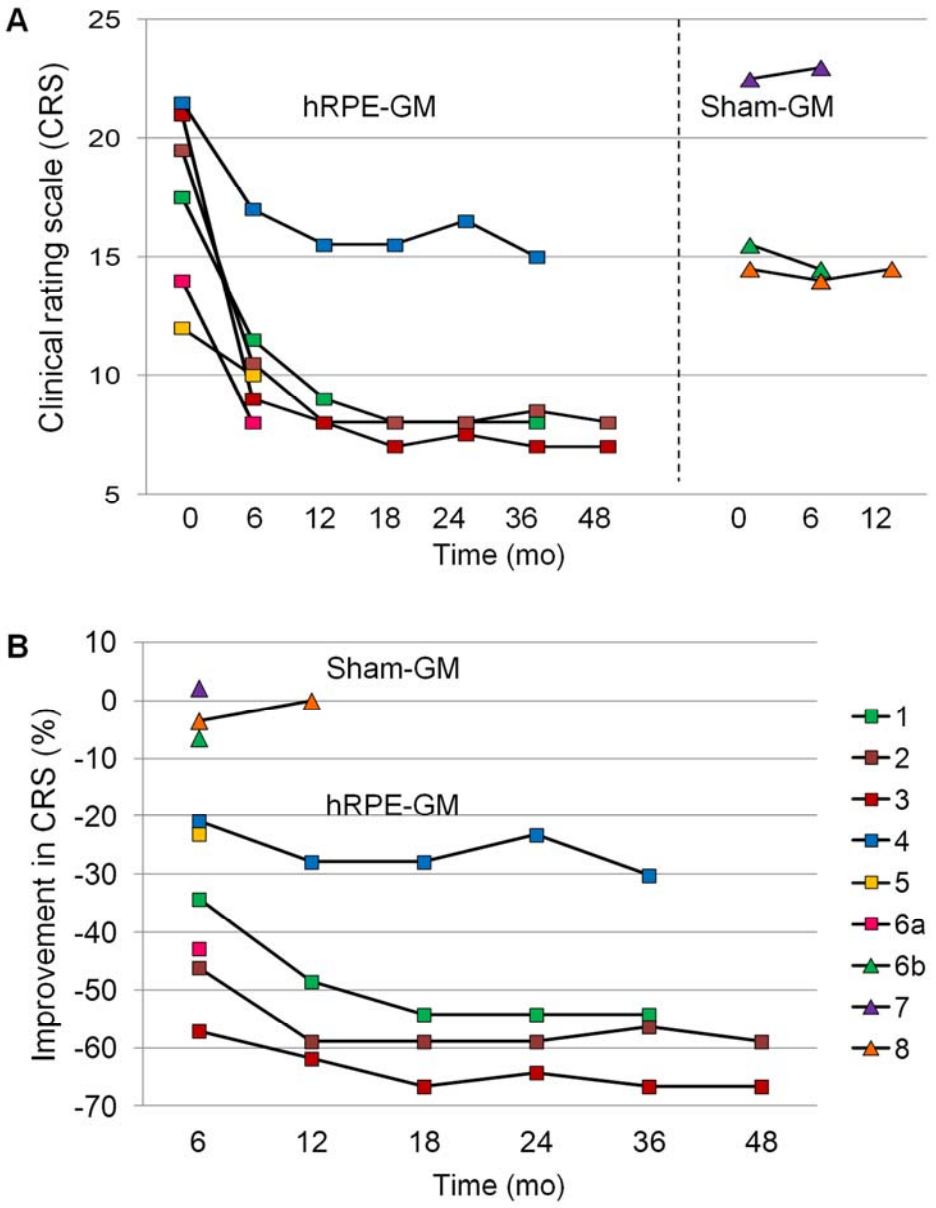

Figure 1. Clinical improvement in individual macaques following cell-based therapy. The hRPE-implanted animals (hRPE-GM: *filled squares*) showed motor recovery from 6 mo to 4 y after unilateral implantation but continued to express mild to moderate bradykinesia and hypokinesia. Maximal benefit was achieved within 1 y and remained stable afterwards. The sham-implanted animals (GM: *filled triangles*) showed no clinical responses. Animal 6 was transplanted sequentially with GM and hRPE-GM in two different hemispheres. [Animals 1-4 received the fetal cells used in the successful phase I trial (*15*) while animals 5-6a received the neonatal cells used in the failed phase II trial (*22*).]

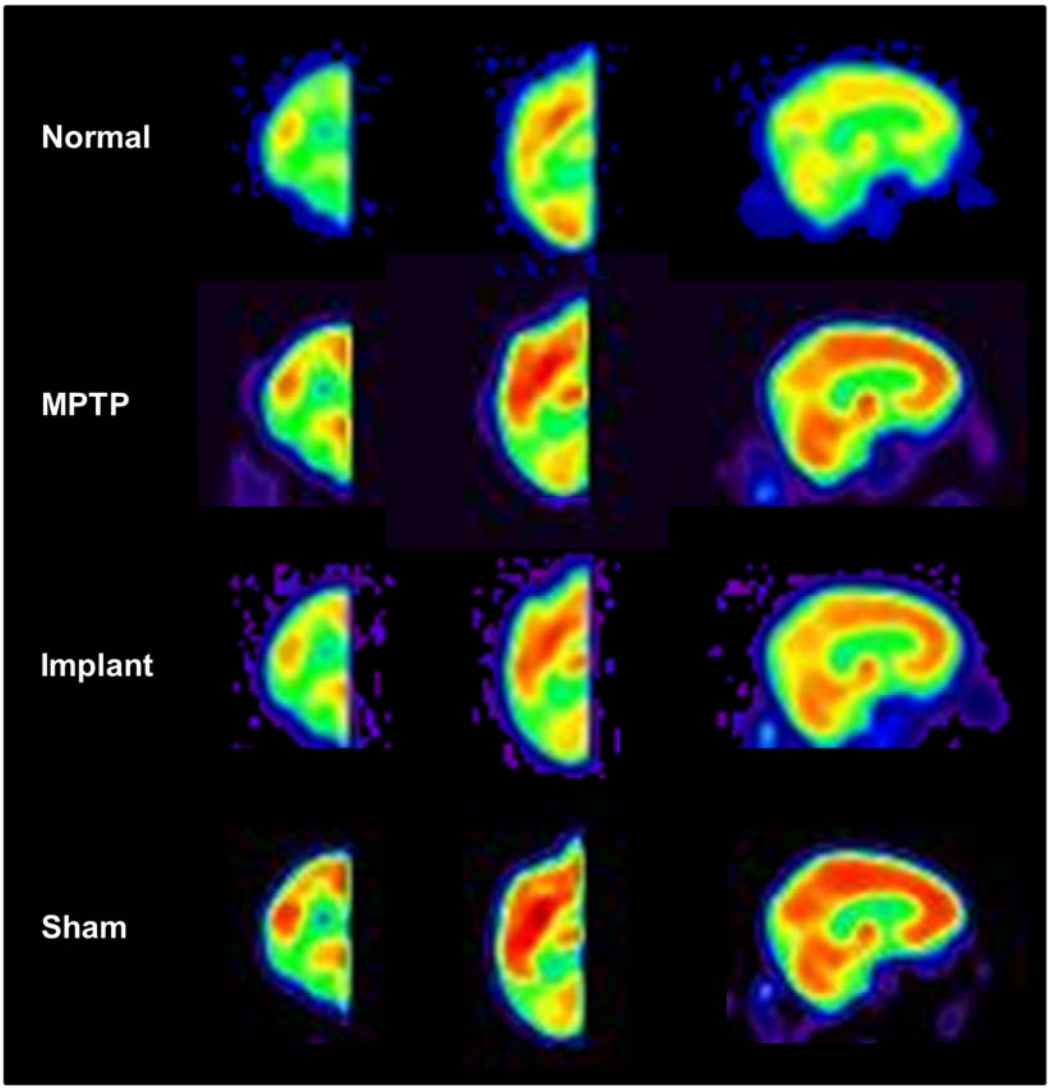

Figure 2. Mean images of relative glucose metabolism in healthy and parkinsonian macaques acquired using a Siemens HRRT scanner. This high resolution PET scanner provides superior image quality for revealing distinct regional differences in cortical and subcortical metabolism among normal, MPTP and hRPE- and sham-implanted hemispheres. [Each image represents brain FDG scans averaged over hemispheres in the individual animal group spatially normalized to a macaque PET brain template (*23*).]

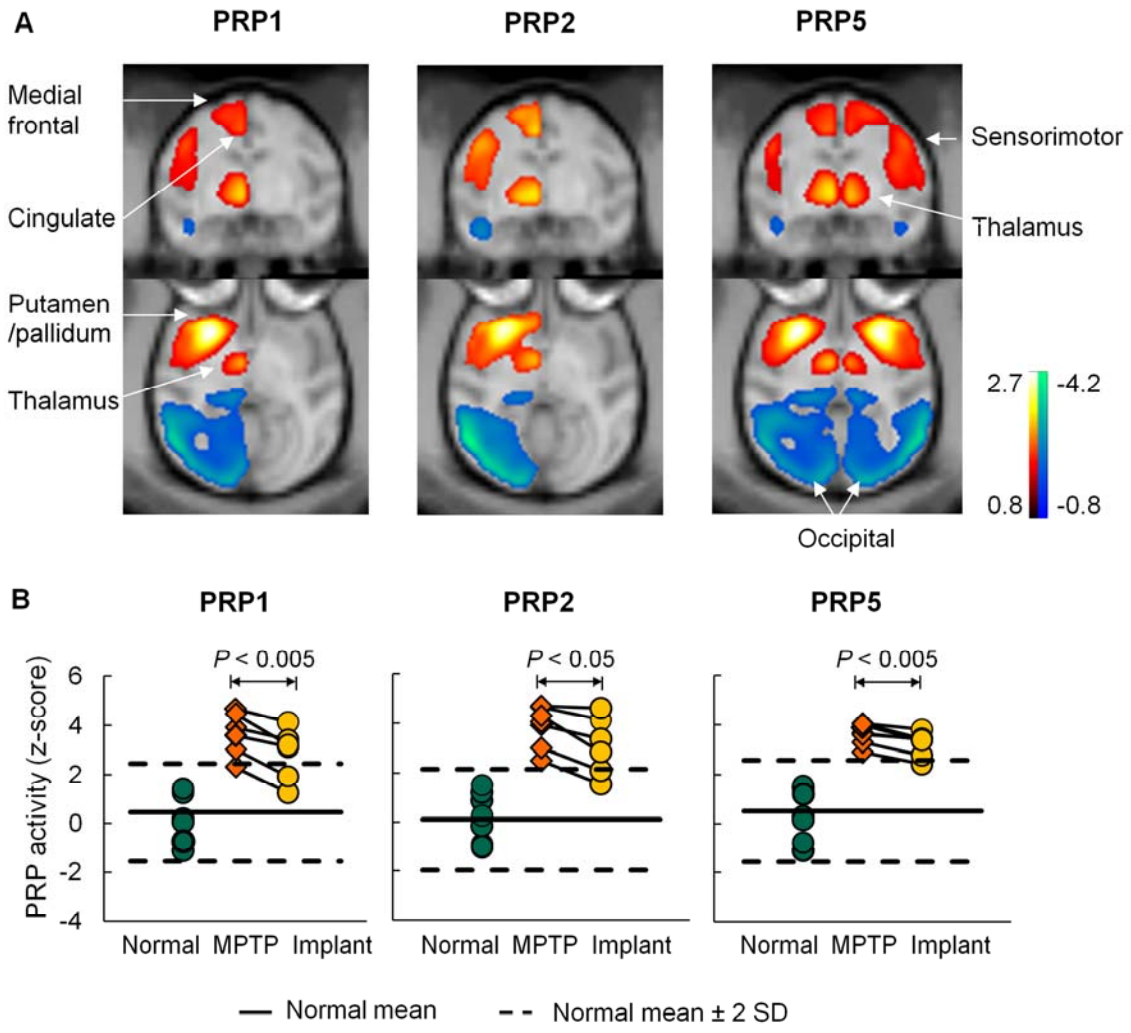

Figure 3. Modulation of abnormal metabolic brain networks in MPTP-induced experimental parkinsonism by hPRE cell transplantation therapy. A. Parkinsonism-related patterns (PRPs) identified on a hemispheric (PRPs 1-2) and whole-brain (PRP 5) basis using FDG PET images in parkinsonian and age-matched healthy macaques (*10*). All PRPs shared analogous topographies with increased (*red to yellow*) and decreased (*blue to green*) metabolic activity in subcortical and cortical regions. B. Network activity in individual hemispheres or brains was elevated ($P < 0.00005$) in the 7 untreated MPTP hemispheres compared to the 8 normal controls, but declined consistently ($P < 0.05$) in the 6 contralateral MPTP hemispheres after hPRE cell implantation. [The patterns are overlaid on a macaque MRI brain template (*23*).]

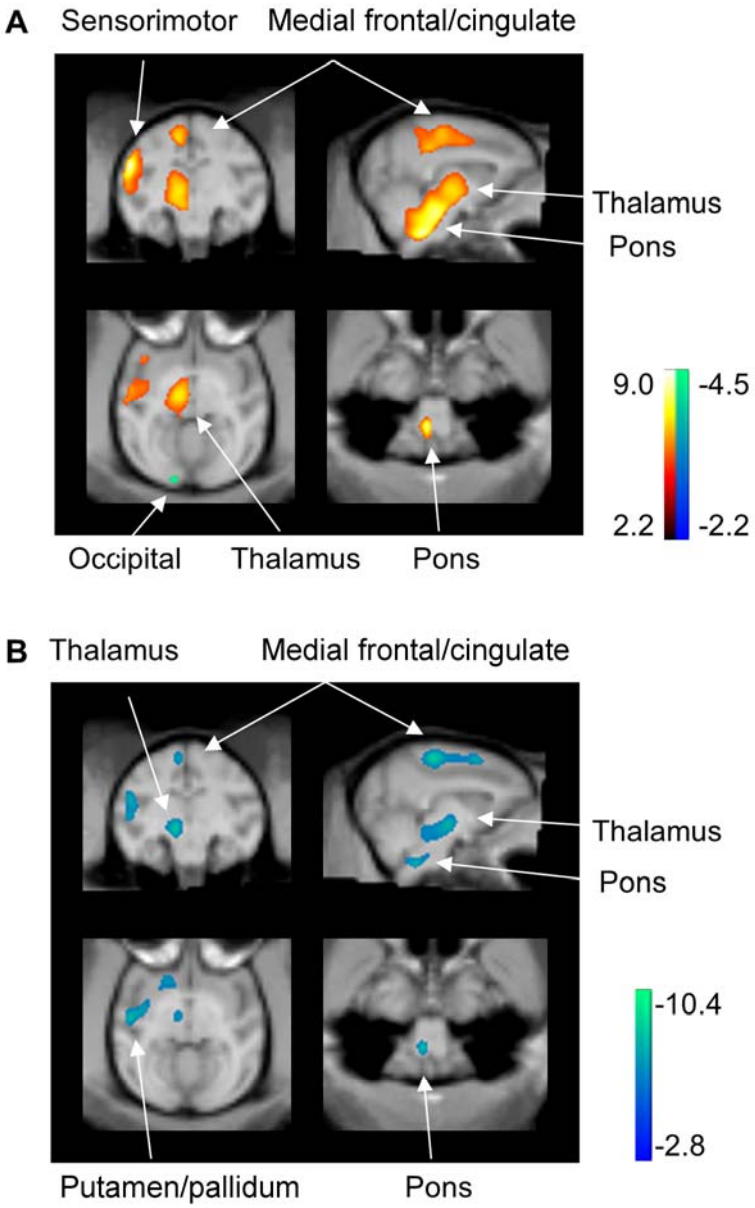

Figure 4. Modulation of abnormal regional metabolism in MPTP-induced experimental parkinsonism by hPRE cell transplantation therapy. A: Metabolism in the 7 untreated MPTP hemispheres increased (*red to yellow*) in a set of subcortical and cortical motor regions relative to the 8 normal controls. B: Metabolism in the 6 hRPE-implanted hemispheres decreased (*blue to green*) in the same set of subcortical and cortical motor regions compared to the 6 untreated MPTP hemispheres. [The SPM *t*-maps of unpaired and paired comparisons are displayed at a lower threshold ($P = 0.025$) for better visualization on a macaque MRI brain template (*23*).]

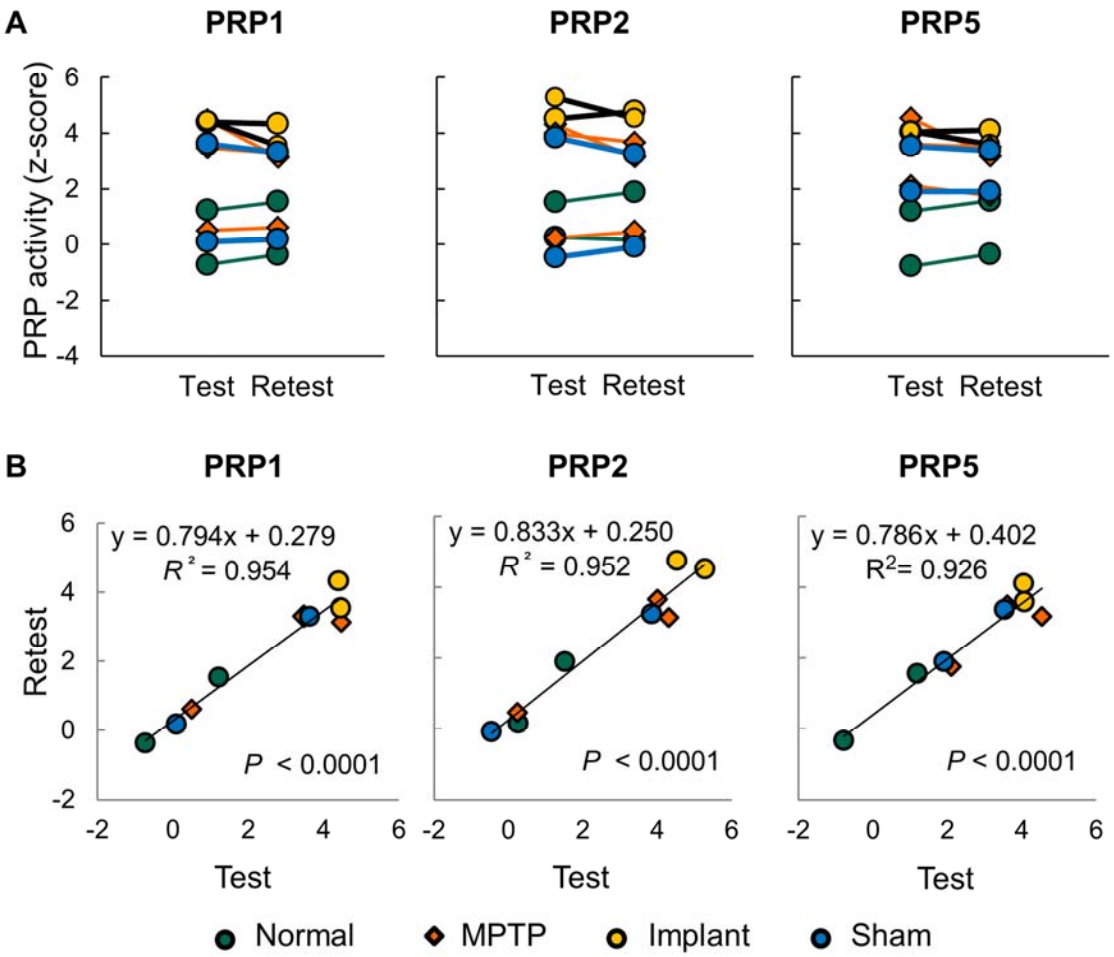

Figure 5. Test-retest reproducibility in PRP network activity. A. Network scores in individual hemispheres or brains were highly reproducible (A: $P > 0.29$) and correlated (B: $R^2 > 0.92$; $P < 0.00005$) between the 9 test and retest scans in the 4 subgroups of 7 macaques. [Network scores were computed on a hemispheric (PRPs 1-2) and whole-brain (PRP 5) basis respectively.]

Table 1: Parkinsonian macaques characteristics and imaging-related parameters

ID	Age (yr)	Weight (kg)	Motor Rating	Dose (MBq)	Glucose (mmol/L)	Condition Left	Condition Right
1	22	9	10	281	4.1	hRPE*	MPTP
2	13	8	8	148	3.7	hRPE*	MPTP
3	13	10	8	185	3.3	hRPE*	MPTP
4	20	10	14	211	3.7	hRPE*	MPTP
5	9	12	10	244	3.6	MPTP	hRPE#
6	14	7	8	185	4.1	hRPE#	GM
7	8	7	23	185	3.5	GM	MPTP
8	9	10	14	222	4.5	MPTP	GM

MPTP, 1-methyl-4-phenyl-1,2,3,6-tetrahydropyridine. * fetal cells; #neonatal cells

Data are provided for the macaques undergoing FDG PET after the unilateral striatal implantation of human retinal pigment epithelial (hRPE) cells or gelatin carriers only (GM) in the left or right striatum.

Table 2: Changes in metabolic network activity under different experimental conditions

	PRP1	PRP2	PRP3	PRP4	PRP5
Pattern Derivation					
Eigenvalue (%)	42.9	43.3	27.8	27.2	48.2
Control 1	0.00 ± 0.41	0.00 ± 0.45	0.00 ± 0.36	0.00 ± 0.33	0.00 ± 0.41
MPTP 1	7.67 ± 1.37	7.91 ± 1.56	3.11 ± 0.25	2.66 ± 0.25	7.78 ± 1.41
MPTP 1 vs Control 1 †	0.0037	0.0031	0.00003	0.00008	0.004
Pattern Validation					
Control 2	0.46 ± 0.36	0.09 ± 0.36	0.22 ± 0.32	0.36 ± 0.28	0.51 ± 0.37
MPTP 2	3.80 ± 0.33	3.88 ± 0.32	3.04 ± 0.22	2.64 ± 0.21	3.64 ± 0.16
MPTP 2 vs Control 2 †	0.00001	0.000003	0.00001	0.00003	0.00002
Implant Effect					
Implant	2.85 ± 0.43	3.10 ± 0.48	2.62 ± 0.39	1.92 ± 0.35	3.21 ± 0.21
Implant vs MPTP 2 (Change %)	-24.6 ± 5.9	-21.6 ± 5.9	-17.6 ± 7.2	-26.8 ± 11.5	-10.9 ± 2.3
Implant vs MPTP 2 ‡	0.0025	0.011	0.036	0.033	0.0039
Implant vs Control 2 †	0.001	0.0003	0.0005	0.004	0.00008
Test-retest Effect					
Test vs Retest ‡	0.292	0.342	0.577	0.505	0.351
R^2 (Pearson Correlation)	0.954	0.952	0.953	0.956	0.926
P	0.000006	0.000007	0.000007	0.000005	0.00003

MPTP, 1-methyl-4-phenyl-1,2,3,6-tetrahydropyridine; PRP, parkinsonism-related pattern. The eigenvalue for each PRP derivation is given as the percent of the total subject × voxel variance (*10*). Subject scores are presented as mean ± standard error for the animals used to identify each PRP and to assess the effects of implantation.

† P values: unpaired Student's *t*-tests.

‡ P values: paired Student's *t*-tests.

Table 3: Brain regions with significant metabolic changes before and after hRPE cell implantation in parkinsonian macaques

Brain regions	Metabolic increase † (MPTP > Normal)					Metabolic decrease ‡ (Implant < MPTP)				
	X	Y	Z	Z_{max}	Size (mm^3)	X	Y	Z	Z_{max}	Size (mm^3)
Medial frontal/Cingulate	8	6	28	3.3	376	4	6	36	2.9	208
Insula/SMC/Putamen	30	16	18	4.9	1304	26	8	18	3.0	744
Frontal/SMA	28	24	18	4.5		26	26	16	3.4	160
Thalamus	6	14	8	2.9	1872	6	14	6	2.8	320
Pons	4	0	−14	3.9		4	0	−14	3.3	184

MPTP, 1-methyl-4-phenyl-1,2,3,6-tetrahydropyridine; SMC, sensorimotor cortex; SMA, supplementary motor area; FDR, false discovery rate.

† Unpaired *t*-test: $P < 0.005$ uncorrected and survived at FDR-corrected $p < 0.05$.
‡ Paired *t*-test: $P < 0.005$ uncorrected and did not survive at FDR-corrected $p < 0.05$.